

Moiré patterns of space-filling curves

Henning U. Voss^{1,2,*} and Douglas J. Ballon²¹*Cornell MRI Facility, Cornell University, Ithaca, New York 14853, USA*²*Department of Radiology, Weill Cornell Medicine, New York, New York 10065, USA*

(Received 25 March 2024; accepted 13 June 2024; published 12 August 2024)

It is shown on the examples of Moore and Gosper curves that two spatially shifted or twisted, preasymptotic space-filling curves can produce large-scale superstructures akin to moiré patterns. To study physical phenomena emerging from these patterns, a geometrical coupling coefficient based on the Neumann integral is introduced. It is found that moiré patterns appear most defined at the peaks of those coefficients. A physical interpretation of these coefficients as a measure for inductive coupling between radiofrequency resonators leads to a design principle for strongly overlapping resonators with vanishing mutual inductance, which might be interesting for applications in MRI. These findings are demonstrated in graphical, numerical, and physical experiments.

DOI: [10.1103/PhysRevResearch.6.L032035](https://doi.org/10.1103/PhysRevResearch.6.L032035)

I. INTRODUCTION

Moiré patterns are interference patterns generated by the overlay of a ruled pattern with transparent gaps on another similar pattern. The spatial scale of a moiré pattern is related to differences of the wave vectors defining the individual patterns and is thus generally larger than that of the individual patterns [1]. The ruled patterns are not necessarily periodic [2], and an averaging process is needed for the accurate identification of a moiré pattern [3]. Two-dimensional space-filling curves were first discovered in 1890 by Peano [4] and are typically ruled patterns. For example, the plane-filling Hilbert curve can be described by very simple iterative rules [5]. Hilbert pointed out that space-filling curves also define a direction of “motion”, forward and backward, in each point of the plane. If one thinks of this motion as a current that flows either way, and connects the two endpoints of such a curve, this defines a magnetic flux through the area enclosed by the curve. In this paper we investigate if pairs of overlaid preasymptotic plane-filling curves exhibit a moiré effect, and what influence the emerging large-scale structures have on the flux coupling between the curves.

The original interest in this work arose from the recently emerging importance of moiré patterns in the electrical properties of twisted graphene bilayers [6] and potential translation into the classical domain. Whereas the present scenario is different, as the moiré patterns emerge from a shift or twist between aperiodic structures with only approximative translational or rotational symmetry, we suggest that the present study can provide insights for the design of interesting

properties of flux-coupled structures, for example in applications such as magnetic resonance imaging (MRI). MRI sensors are quite generally made of electromagnetic resonator arrays confined to a surface, and the understanding of electromagnetic coupling between array elements plays a crucial role in their engineering [7–11]. Notably, the recently discovered concept of topological modes can arise both in coupled resonator systems [12] as well as in twisted bilayers [13].

The organization of this article is as follows: First, the moiré effect is demonstrated in two different space-filling curves: Spatially shifted Moore curves, and twisted Gosper curves. These two examples represent curves with approximate translational and rotational symmetry, respectively. Next, the Neumann integral is introduced as a geometric measure of distance in space-filling curves, and it is shown that its value peaks at those shifts or twists with the most defined moiré effect. We then demonstrate in a physical experiment that the interpretation of the Neumann integral as a measure for inductive coupling in radiofrequency resonators leads to design rules for strongly overlapping space-filling resonators with vanishing mutual inductance. Finally, limitations of the Neumann integral formulation and potential applications are discussed.

II. GRAPHICAL EXPERIMENTS: MOIRÉ PATTERNS OF THE MOORE AND GOSPER CURVES

In the first graphical experiment, we investigate the large-scale structures emerging from preasymptotic Moore curves [Fig. 1(a)]. The Moore curve is a generalization of the Hilbert curve. In the Hilbert curve, the start and end points are at different corners, and the Moore curve brings them next to each other by stitching four Hilbert curves together. Connecting start and end points then forms a closed loop, such that current passing through it will induce a magnetic flux.

Moore curves were generated with MATLAB (The Mathworks, version R2023a), using a Lindenmayer algorithm [14,15]. MATLAB code used to generate this and the

*Contact author: hv28@cornell.edu

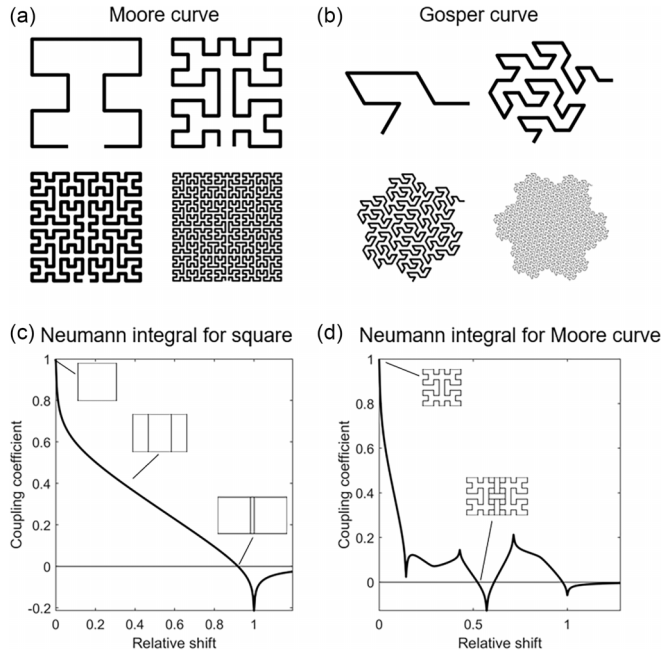


FIG. 1. Space filling curves and Neumann integrals. (a) The first four iterations of the Moore curve. (b) The first four iterations of the Gosper “snowflake” curve. (c) The Neumann integral for shifted squares ($\Delta = 0.001$). Square resonators have vanishing inductive coupling at a relative shift of about 0.92. (d) The Neumann integral for shifted Moore curves with $N_i = 2$ ($\Delta = 0.01$). Moore resonators with $N_i = 2$ have vanishing inductive coupling at relative shifts of 0.52, 0.61, and 0.97.

following figures is available on request from the authors. The number of iterations of the Lindenmayer system was $N_i = 7$. Figure 2 shows examples of the moiré effect in these curves. For certain shifts, superstructures emerge, consisting of relatively bright parts that locally resemble the original Moore curves and darker parts that appear more complex. This is being emphasized in the magnified insets. The down-sampling of the pattern to publication resolution here acted as an averaging filter, and no additional averaging was necessary.

The second example demonstrates the moiré effect in space-filling curves exhibiting approximate rotational rather than translational symmetry. We chose the Gosper “snowflake” curve [Fig. 1(b)] [16], which has 30° and 60° intrinsic angles that follow from the curve’s construction by connecting nodes of a hexagonal lattice. In this case of rotational symmetry, it is natural to anticipate twisted moiré patterns. Figure 3 shows examples for the moiré effect in Gosper curves with $N_i = 6$ for selected twist angles. This visualization required additional averaging; the patterns were smoothed with a disk-shaped “pillbox” averaging filter, and the display range was adjusted for enhanced contrast. For certain angles, superstructures with approximate sixfold and threefold symmetries emerge.

III. NUMERICAL EXPERIMENTS: COUPLING ANALYSIS OF MOIRÉ PATTERNS

The Neumann integral [17] is a geometric measure [18] of distance between curves with the property that the

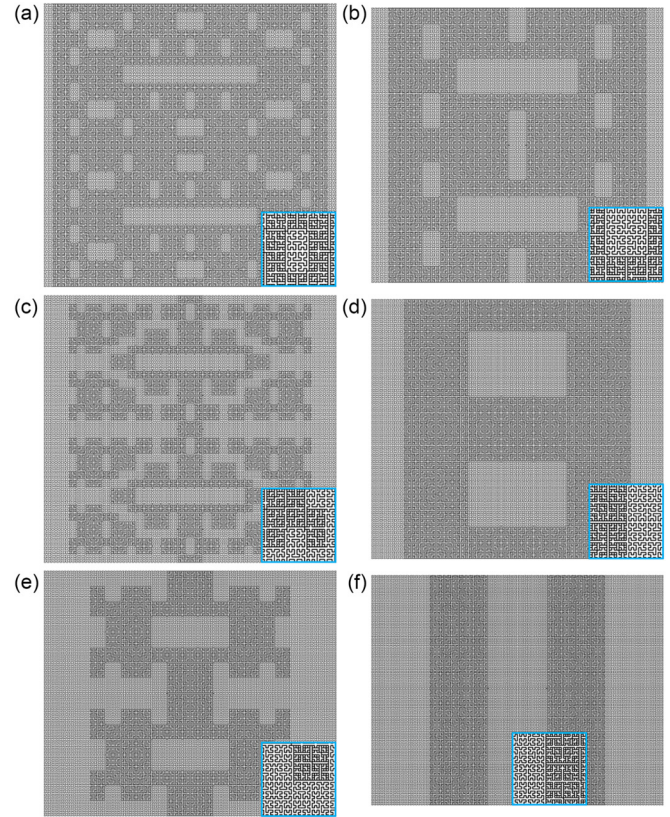


FIG. 2. Moiré effect in space-filling Moore curves. The relative spatial shifts of the two Moore curves are (a) 3.1%, (b) 6.3%, (c) 9.4%, (d) 13%, (e) 19%, (f) 25%. Each curve is shown with a magnified inset to reveal its details.

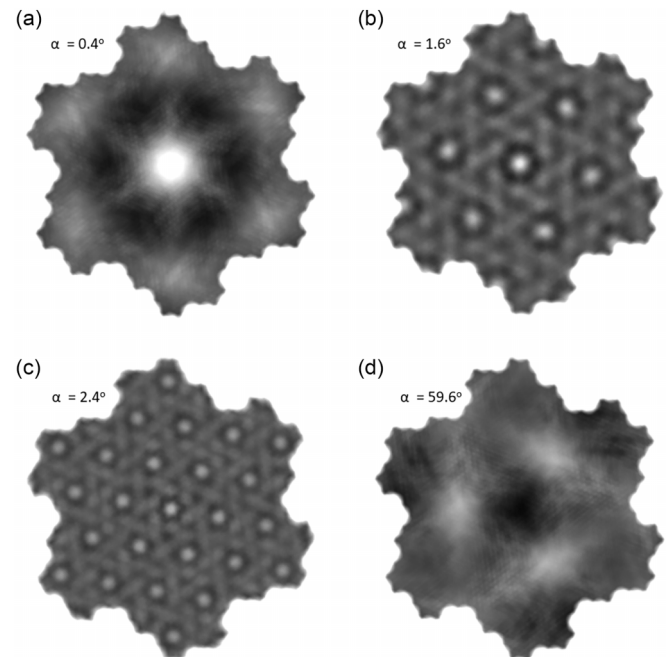


FIG. 3. Moiré effect in space-filling Gosper curves for selected rotation angles.

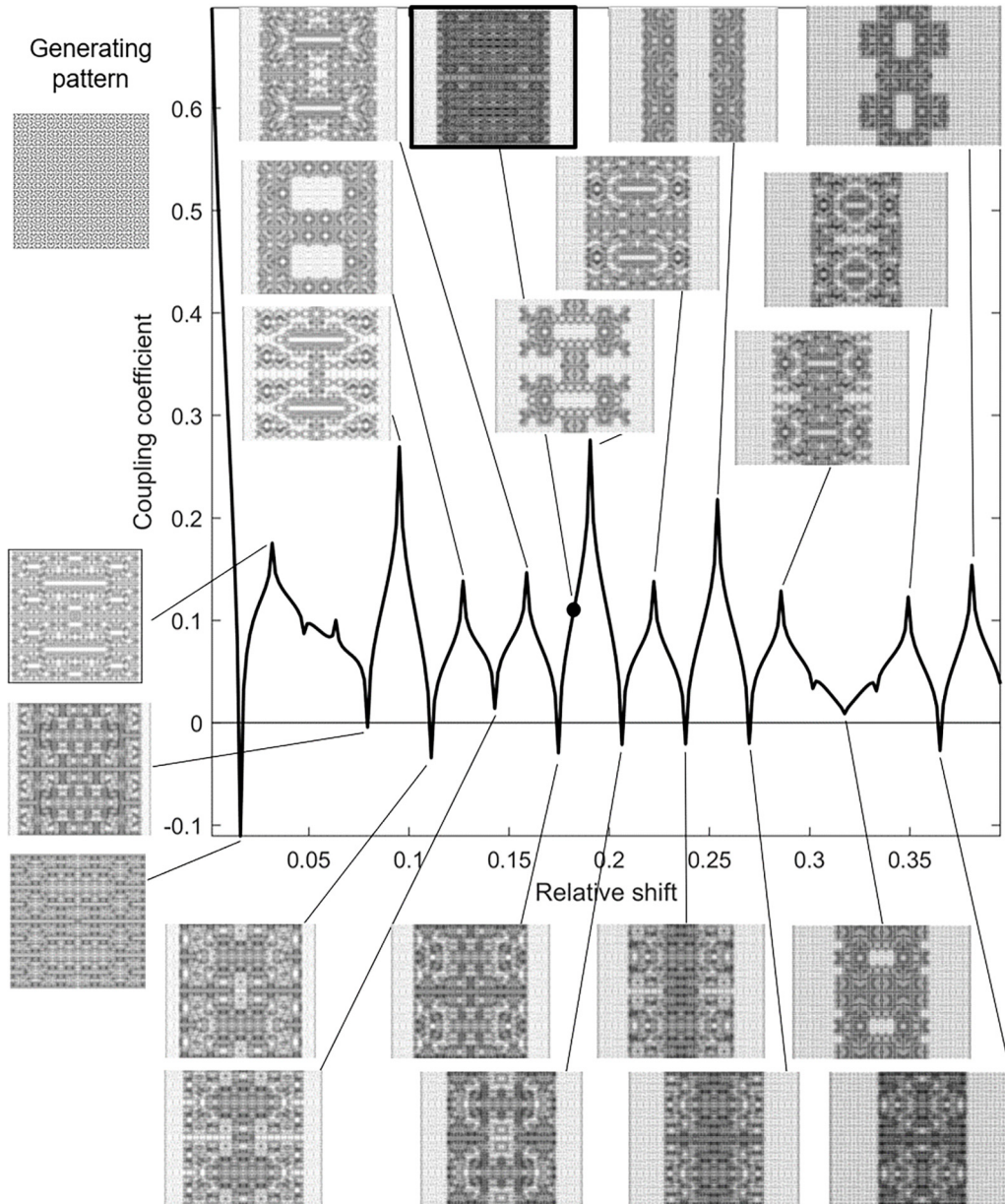


FIG. 4. Coupling coefficients of two shifted Moore curves for the fifth iteration towards the space-filling curve, as a function of the relative spatial shift. In addition, some of the resulting patterns are shown. The moiré effect appears most defined at the peaks of the coupling coefficients. For the framed pattern, located in-between two peaks, large scale structures are not clearly as discernible anymore.

directionality of the curve is taken into account. This property corresponds to the aforementioned “motion” directionality in space-filling curves by Hilbert. With proper physical scaling, the Neumann integral approximates the mutual inductance between two closed loops made of thin wires with radius negligible compared to their lengths. The normalized Neumann integral provides a direct estimate of the inductive coupling coefficient, a dimensionless quantity that will be used here.

The normalized Neumann integral for our application of two spatially offset in-plane curves is defined as

$$\zeta_{\alpha} = \frac{1}{N_0} \oint_{C_1} \oint_{C_2(\alpha)} \frac{d\mathbf{r}_1 \cdot d\mathbf{r}_2}{|\mathbf{r}_1 - \mathbf{r}_2|}, \quad (1)$$

where C_1 and C_2 are the curves defined by the conductors, α is the shift distance or twist angle between the two curves, and $d\mathbf{r}_1$ and $d\mathbf{r}_2$ are the infinitesimal increments of vectors \mathbf{r}_1 and \mathbf{r}_2 defining the curves. It is assumed that the two curves have a small, constant offset Δ perpendicular to the plane to avoid divergence for $\alpha = 0$ and to provide a realistic approximation for conductors on a substrate with finite thickness. The normalization constant N_0 is obtained by the same double line integral for $\alpha = 0$.

The notion of the Neuman integral as a geometric distance measure is illustrated here on two identical square loops in the plane, of which one of them has a small spatial offset Δ . Neumann integrals were computed with MATLAB by dividing the loops into line elements and estimating the integral as the sum over the resulting piecewise-linear integrands.

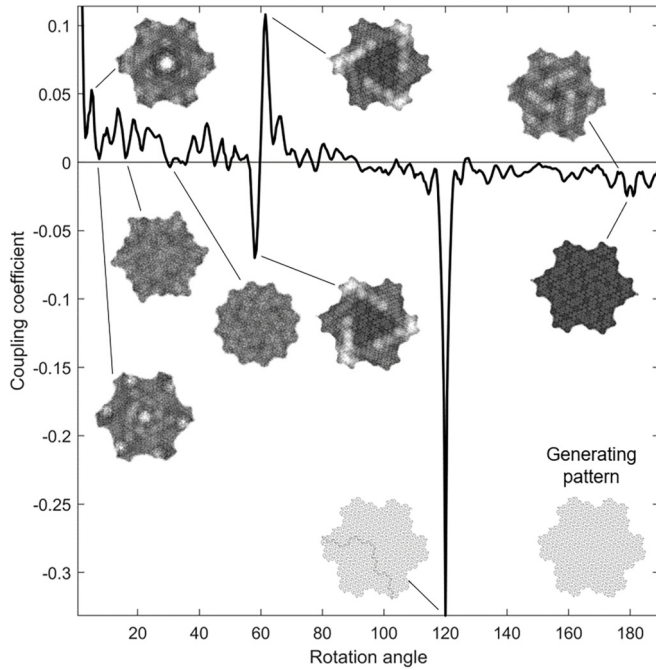


FIG. 5. Coupling coefficients of two twisted Gosper curves for the fourth iteration towards the space-filling curve, as a function of the rotation angle from 5° to 190° . In addition, some resulting patterns, including moiré patterns, are shown.

Computation was accelerated by parallel computation using ten cores. If the square loops are overlapping completely ($\alpha = 0$), the normalized Neumann integral ζ_α is one. It decreases for larger α and vanishes once it reaches a point of little overlap at a relative shift of $\alpha = 0.92$, before it becomes negative [Fig. 1(c)]. For larger α , it asymptotically vanishes again. The physical interpretation of this graph is as follows. If the two squares define wires (of inductance L) with an inserted capacitor (of capacitance C), they model two individual LC resonators that are inductively coupled to each other. Generally, if the two resonators are facing each other in a solenoidal configuration, their coupling (or mutual inductance entering the Kirchhoff equations, including its sign) is positive. If they are oriented in the same plane as in the figure without overlap, their coupling is negative. Upon bringing the loops closer together their coupling first increases in magnitude but finally decreases until it vanishes at $\alpha = 0.92$ [7]. To understand this behavior, one can simply consider magnetic flux lines emanating from the left loop upwards; if there is a large overlap of the two loops, most flux lines enter the right loop in upward direction, too. For larger shift, or decreasing overlap, the flux lines from the left loop ultimately reverse sign, now entering the right loop from above. These two cases are modeled by a positive and negative coupling coefficient, respectively. The Neumann integrals for two shifted Moore curves are markedly different from the case of two shifted squares [Fig. 1(d)]. This will be explored in the following.

Figure 4 shows the computed coupling coefficient of two spatially shifted Moore curves ($N_i = 5$, $\Delta = 0.01$) as a function of the relative shift α . The Neumann integral or coupling coefficients attain both positive and negative values, and their

graph has pronounced peaks. The insets depict selected moiré patterns of the two overlaid Moore curves, after smoothing with a box averaging filter and contrast enhancement. Most pronounced moiré effects occur at the peaks of the coupling.

Figure 5 shows the computed coupling coefficient of two twisted Gosper curves ($N_i = 4$, $\Delta = 0.001$) as a function of the twist angle α , with some selected moiré patterns. The coupling is symmetric around $\alpha = 180^\circ$, and values for $\alpha > 190^\circ$ are not shown. The rotation center was chosen such that for $\alpha = 120^\circ$ maximum congruence of the two curves was achieved. Except for the pattern at 120° rotation angle, which does not show a moiré effect, the moiré patterns were smoothed with a pillbox averaging filter. Overall, the coupling coefficients change in a more complex way with α than in the Moore curve. It was also observed that the curve depends more sensitively on the value of the distance Δ .

IV. PHYSICAL EXPERIMENT: COUPLED RESONATORS

For experimental testing of the preceding model simulations, the Moore curve was chosen due to its simpler coupling coefficient behavior under changing spatial shift compared to the more complex Gosper curve's behavior under changing twist angle.

Two Moore radiofrequency resonators with $N_i = 3$ and dimension 7.5×7.5 cm were fabricated on a printed circuit board with 1.7-mm thickness and an insulation layer above the copper traces [Fig. 6(a)]. A 10 pF-capacitor (measured value 11.7 pF) was inserted serially into one of the corners of the first Moore curve, and a variable capacitor of 20 pF into the second Moore curve. On the first circuit, the measured resistance was 0.63Ω , and the resonance frequency 55.0 MHz. The second circuit's resonance frequency was matched to the one of the first circuit. The two circuit boards were then aligned while facing each other ($\Delta = 0.2$ mm). The S_{11} reflection coefficient spectrum of the coupled Moore resonators was measured with a network analyzer (NanoVNA H2/H4, Taobao, Hangzhou, China) for shifts from 17% to 110%, using an inductively coupled pickup loop of about the same size as the resonators. Mode splitting of two coupled LC radiofrequency resonators is expected to be $\omega_{1,2} = \sqrt{(1 \mp \kappa)LC}^{-1}$, from which the coupling coefficient follows as $\kappa = \frac{\omega_1^2 - \omega_2^2}{\omega_1^2 + \omega_2^2}$. Due to resistance, modes have a finite linewidth, here found to be $Q = \omega/\Delta\omega = 55$, and zero-coupling shifts were defined as those for which a visible split of resonances could not be observed.

The numerically estimated Moore curve coupling coefficients are shown in Fig. 6(b), black graph. Experimentally, the shift between the two boards was gradually increased, and the resonance frequencies were obtained from the S_{11} spectrum. From the resonance frequencies, the coupling coefficients κ were computed [Fig. 6(b), red graph]. When the two resonances could not be isolated, the $\kappa = 0$ condition is satisfied. This is demonstrated in the first and third insets, which show S_{11} spectra with only one resonance. The second and fourth insets provide examples for S_{11} spectra with split resonances due to nonzero coupling. Overall, the measurements are in good agreement with the numerical values. Experimental factors such as finite copper trace widths, finite line widths due to

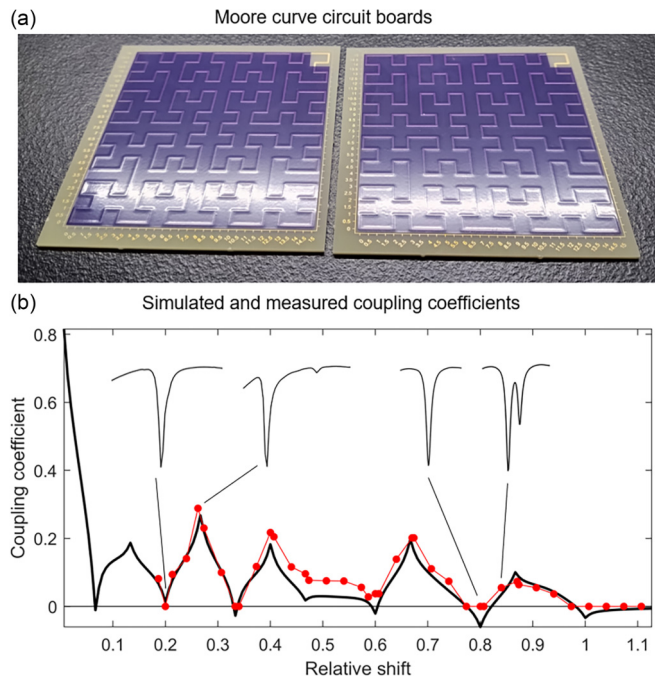


FIG. 6. Physical experiment of coupling in Moore resonators. (a) The copper layers on two printed circuit boards define two Moore curves with $N_i = 3$. After the addition of a capacitor (not shown) they become radiofrequency resonators. (b) Observed coupling coefficients (red) vs Neumann integral simulation (black) for shifted circuit boards. The insets provide examples for single resonances, or zero coupling (first and third inset), and resonance splitting due to inductive coupling (second and fourth inset).

resistance, and finite measurement resolution of the network analyzer might contribute to remaining deviations from theory. The near-zero coupling point at relative shifts of about 0.47 could not be isolated with this experiment. In summary, approximate zero coupling could be achieved for significantly overlapping Moore resonators at multiple shift values.

V. DISCUSSION

Space-filling curves are not only of mathematical interest but have found application in various fields of science and engineering. For example, they have been utilized for decades to study the folding principles of proteins and polymers [19].

Hilbert and Moore curves have been suggested as solutions to build miniature antennas by compressing long wires into small areas [20,21]. Our interest is in potential applications as radiofrequency resonators. Radiofrequency resonator arrays are the main component of MRI phased arrays [7], for which one usually tries to minimize coupling. In phased arrays, it is important to understand the effects of coupling on the resonance spectra and eigenmodes of the arrays. Sometimes, inductive coupling is even desired in MRI coils such as high-pass surface resonator arrays [9]. The Neumann integral approximates the mutual inductance between closed wire loops under certain conditions, such as thin wires, smoothness, no concave areas, and low frequencies [18]. These conditions are only partially fulfilled in space-filling curve geometries [22,23] and MRI applications, and would introduce systematic errors in estimates of mutual inductance. Nevertheless, this does not affect the use of the Neumann integral as a geometric distance measure; as we have shown, the Neumann integral peaks at the emergence of moiré patterns, and if used as an estimate of mutual inductance, can indeed predict vanishing inductive coupling configurations of space-filling radiofrequency resonators.

VI. SUMMARY

It has been demonstrated that preasymptotic space-filling curves naturally lead to moiré patterns. Moiré patterns emerge in shifted space-filling curves with approximate translational symmetry as well as in twisted space-filling curves with approximate rotational symmetry. The Neumann integral was used as a geometric distance measure between two space-filling curves, and it was shown that it peaks at those shifts or twists that cause a pronounced moiré effect. Furthermore, if interpreted as a measure of inductive coupling, the Neumann integral also predicts zero-coupling configurations of space-filling radiofrequency resonators, an important design criterion for potential MRI applications.

ACKNOWLEDGMENTS

We thank a reviewer pointing out the role of averaging in the moiré effect.

The authors are inventors on patents, owned by Cornell University, that are related to radiofrequency resonators akin to those in this manuscript.

- [1] I. Amidror, *The Theory of the Moiré Phenomenon - Volume I: Periodic Layers* (Springer, Berlin, 2007).
- [2] I. Amidror, *The Theory of the Moiré Phenomenon - Volume II: Aperiodic Layers* (Springer, Berlin, 2007).
- [3] V. Saveljev, *The Geometry of the Moiré Effect in One, Two, and Three Dimensions* (Cambridge Scholars Publishing, Cambridge, 2022).
- [4] G. Peano, Sur une courbe, qui remplit toute une aire plane, *Math. Ann.* **36**, 157 (1890).
- [5] D. Hilbert, Ueber die stetige abbildung einer linie auf ein flächenstück, *Math. Ann.* **38**, 459 (1891).
- [6] Y. Cao *et al.*, Unconventional superconductivity in magic-angle graphene superlattices, *Nature (London)* **556**, 43 (2018).
- [7] P. B. Roemer, W. A. Edelstein, C. E. Hayes, S. P. Souza, and O. M. Mueller, The NMR phased-array, *Magn. Reson. Med.* **16**, 192 (1990).
- [8] D. Ballon and K. L. Meyer, Two-dimensional ladder network resonators, *J. Magn. Reson. Ser. A* **111**, 23 (1994).
- [9] H. U. Voss and D. J. Ballon, High-pass two-dimensional ladder network resonators for magnetic resonance imaging, *IEEE Trans. Biomed. Eng.* **53**, 2590 (2006).

- [10] R. Brown, Y. Wang, P. Spincemaille, and R. F. Lee, On the noise correlation matrix for multiple radio frequency coils, *Magn. Reson. Med.* **58**, 218 (2007).
- [11] P. Spincemaille, R. Brown, Y. X. Qian, and Y. Wang, Optimal coil array design: The two-coil case, *Magn. Reson. Imaging* **25**, 671 (2007).
- [12] H. U. Voss and D. J. Ballon, Topological modes in radiofrequency resonator arrays, *Phys. Lett. A* **384**, 126177 (2020).
- [13] M. I. N. Rosa, M. Ruzzene, and E. Prodan, Topological gaps by twisting, *Commun. Phys.* **4**, 130 (2021).
- [14] A. Lindenmayer, Mathematical models for cellular interactions in development II. Simple and branching filaments with two-sided inputs, *J. Theor. Biol.* **18**, 300 (1968).
- [15] L. C. Ting, Compute the fractal curve based on the following L system, <https://www.mathworks.com/matlabcentral/answers/38785-matlab-compute-moore-curve-help> (2012).
- [16] M. Gardner, Mathematical Games—In which “monster” curves force redefinition of the word “curve”, *Sci. Am.* **235**, 124 (1976).
- [17] F. E. Neumann, *Die Mathematischen Gesetze der Inducirten Elektrischen Ströme* (W. Engelmann, Leipzig, Germany, 1889).
- [18] K. L. Corum and J. F. Corum, RF coils, helical resonators and voltage magnification by coherent spatial modes, in *Proceedings 5th International Conference on Telecommunications in Modern Satellite, Cable and Broadcasting Service, Telsiks 2001, Nis, Yugoslavia* (IEEE, Piscataway, NJ, 2001), Vols. 1 and 2, pp. 339–348.
- [19] N. Kinney, M. Hickman, R. Anandakrishnan, and H. R. Garner, Crossing complexity of space-filling curves reveals entanglement of S-phase DNA, *PLoS ONE* **15**, e0238322 (2020).
- [20] H. A. Wheeler, Fundamental limitations of small antennas, in *Proceedings of the Institute of Radio Engineers* (IEEE, New York, 1947), p. 181.
- [21] J. M. González-Arbesú, S. Blanch, and J. Romeu, Are space-filling curves efficient small antennas? *IEEE Antennas Wirel. Propag. Lett.* **2**, 147 (2003).
- [22] D. L. Jaggard, Fractal electrodynamics and modeling, *Directions in Electromagnetic Wave Modeling* (Springer, New York, 1991), pp. 435–446.
- [23] M. J. Ogorzalek, Fundamentals of fractal sets, space-filling curves and their applications in electronics and communications, *Intelligent Computing Based on Chaos* (Springer, New York, 2009), p. 53.